

# Highly Sensitive Detection of Cancer Biomarker EGFR by PicoTREC-SERS

Lifu Xiao<sup>1</sup>, Sitaram Harihar<sup>2</sup>, Yangzhe Wu<sup>1</sup>, Danny R Welch<sup>2</sup>, Anhong Zhou<sup>1,\*</sup>

<sup>1</sup>Department of Biological Engineering, Utah State University, Logan, Utah, USA

<sup>2</sup>Department of Cancer Biology, The Kansas University Medical Center, Kansas City, USA

Tel: (435)79792863; Fax: (435)7970148; Email: Anhong.Zhou@usu.edu

## ABSTRACT

Epidermal growth factor receptor (EGFR) plays an important role in signaling pathway of the development of breast cancer cells. Since EGFR overexpresses in most breast cancer cells, it is regarded as a biomarker molecule of breast cancer. Here, two model breast cancer cell lines expressing different levels of EGFR, MDA-MB-435 and MDA-MB-231, and their Breast cancer Metastasis suppressor (BRMS1) expressing counterparts, i.e., MDA-MB-435<sup>BRMS1</sup> and MDA-MB-231<sup>BRMS1</sup>, were used to demonstrate the competence of SERS and AFM PicoTREC in the applications of detection of EGFR on single cells. Our preliminary data show that: (1) spatial distribution of EGFR on single breast cancer cells measured by gold nanorod based SERS; (2) single-molecular distribution of EGFR on single breast cancer cells measured by AFM PicoTREC; (3) BRMS1 differently regulate EGFR expression on MDA-MB-435 and MDA-MB-231.

**Keywords:** EGFR, PicoTREC, SERS, BRMS1

## 1 INTRODUCTION

It is reported that for women in the U.S., breast cancer death rates are higher than those for any other cancer, besides lung cancer. Considering the fact that approximately 70–80% of breast carcinomas overexpress the epidermal growth factor receptor (EGFR)<sup>1</sup> and that the cell surface EGFR represents a current major therapeutic target to treat breast cancer (i.e., anti-EGFR therapy treatment), there is an urgent need to develop an ultrasensitive technique to detect EGFR at the single molecule level on breast cancer cells. Up to now, it's not clear about spatial distribution and/or distribution pattern of EGFRs on the single cell level.

Surface-enhanced Raman spectroscopy (SERS) is a powerful analytical tool for biological applications, especially in ultrasensitive detection of single molecule. It turns the weak inelastic scattering effect of photons into a structurally sensitive single-molecule and nanoscale probe<sup>2</sup>, allowing ultra-detection and non-invasive tagging of specific bioanalytes in living cells and animals<sup>3</sup>. Atomic force microscopy (AFM) based PicoTREC (simultaneous Topography and RECOgnition imaging) technique, in which a cantilever tip carries a probe molecule that recognizes the

analyte of interest, has been developed for cell surface receptor imaging with high spatial and temporal resolution<sup>4</sup>.

BRMS1 gene is a member of metastasis suppressors, which inhibit metastasis without blocking orthotopic tumor formation at any step of the metastatic cascade. BRMS1 has been shown to regulate phosphoinositide signaling<sup>5</sup>, expression of EGFR<sup>6</sup>, osteopontin<sup>7</sup>, NFκB<sup>8</sup>, and connexins<sup>9</sup>, all of which have been known to play significant roles in cancer progression.

In this work, breast cancer cells, MDA-MB-435 and MDA-MB-231, and their BRMS1 expressing counterparts, MDA-MB-435<sup>BRMS1</sup> and MDA-MB-231<sup>BRMS1</sup>, were used to demonstrate the competence of AFM PicoTREC and SERS in the applications of detection of EGFR on single cells. In addition, the effect of BRMS1 on EGFR expression in MDA-MB-435 and MDA-MB-231 cells was also studied.

## 2 MATERIALS AND METHODS

Gold Nanorods (GNRs) for SERS measurements were purchased from Nanopartz Inc. (USA). SERS spectra and images were collected by a Renishaw inVia Raman spectrometer (Renishaw, UK) connected to a Leica microscope (Leica DMLM, Leica Microsystems, USA), equipped with a 785 nm near-IR laser that was focused through a 63x water immersion objective (NA+0.90, Leica Microsystems). SERS spectra and image processing was performed using Renishaw WiRE 3.3 software.

For AFM PicoTREC measurements, magnetically coated silicon nitride AFM tips were functionalized with antibody using the method reported previously<sup>4</sup>. AFM recognition imaging was performed on a PicoPlus AFM system with a commercially available electronic attachment (PicoTREC, Agilent Technologies, AZ). Image processing was performed using PicoView 10.1 software (Agilent Technologies).

Human breast cancer cell lines (A431, MDA-MB-435, MDA-MB-231, 435<sup>BRMS1</sup> and 231<sup>BRMS1</sup>) were grown in a 1:1 mixture of Dulbecco's-modified eagle's medium (DMEM) and Ham's F-12 medium supplemented with 5% fetal bovine serum in a humidified atmosphere at 37 °C with 5% CO<sub>2</sub>. Cells (approximately 10<sup>6</sup> cells/ml) were passaged at 80–90% confluency prior to experiments.

### 3 EXPERIMENTAL RESULTS

#### 3.1 SERS Detection of EGFR

In this work, we designed a SERS probe based on polyelectrolyte-coated gold nanorods (GNRs) to detect breast cancer cells by specifically recognizing EGFR molecules (via antibody-antigen interaction) on the cell surface membrane. The synthesis of the SERS probe includes 3 steps (Fig. 1A): (1) bare GNRs were conjugated to 4-mercaptobenzoic acid (MBA) via Au-S bonds; (2) poly(allylamine hydrochloride) (PAH) were coated on MBA-GNRs; (3) the GNRs were functionalized by monoclonal antibody anti-EGFR. The size and morphology of the SERS probes were visualized by TEM (Fig. 1B). The successful coating of PAH and antibody is confirmed by a thin dim film on the surface of GNRs. Here, MBA is used as Raman reporter molecules to optimize SERS sensitivity due to its strong affinity to Au surface and simple SERS spectrum (characteristic Raman band at  $1077\text{ cm}^{-1}$ ). The PAH molecule, a polyelectrolyte with positive charge, is playing important roles not only preventing the GNRs from aggregation, but also providing biocompatibility to the SERS probes. Fig. 1C shows the UV-vis spectra of the GNRs at each steps of the preparation process. The longitudinal plasmon resonance band for bare GNRs is located at  $770\text{ nm}$ , which is related to the 3.7 aspect ratio of the nanorods (Fig. 1B). After the coatings of MBA, PAH and antibody, the longitudinal plasmon band maxima redshifted a little bit ( $\sim 5\text{ nm}$ ), which is probably due to the changes in the local refractive index after chemicals coating.

In order to investigate whether the anti-EGFR functionalized SERS probe can successfully detect the expression of EGFR on the overexpressing cells, a competitive inhibition test was performed using a breast cancer cell line A431, expressing high levels of EGFR on cell membrane<sup>10</sup>. A431 cells were incubated with the SERS probe under two different conditions: (1) A431 cells were incubated with the probe for 1h at  $37\text{ }^{\circ}\text{C}$  (Control); (2) as a competitive inhibition test, A431 cells were pre-blocked with free anti-EGFR antibody for 1h and then incubated with the probe for 1h (Block). The typical SERS spectra for Control and Block groups are shown in Fig. 1D. The Control group shows intense peaks at  $1077\text{ cm}^{-1}$  and  $1588\text{ cm}^{-1}$ , while there is no obvious Raman peak in the spectrum of Block group. Furthermore, our results show that the Raman intensities at  $1077\text{ cm}^{-1}$  for Control group is significantly higher ( $P < 0.001$ ,  $n = 60$ ) than that for Block group (Fig. 1E). These results confirm that SERS signals on A431 cells resulted from the recognition of EGFR by the specific antibody-antigen interaction, but not the non-specific adsorption. The drastic decrease in SERS signals in the Block group is because the free anti-EGFR antibody blocked the receptors on the cell membrane so that the SERS probes were unable to bind with the receptors on the cell surfaces.

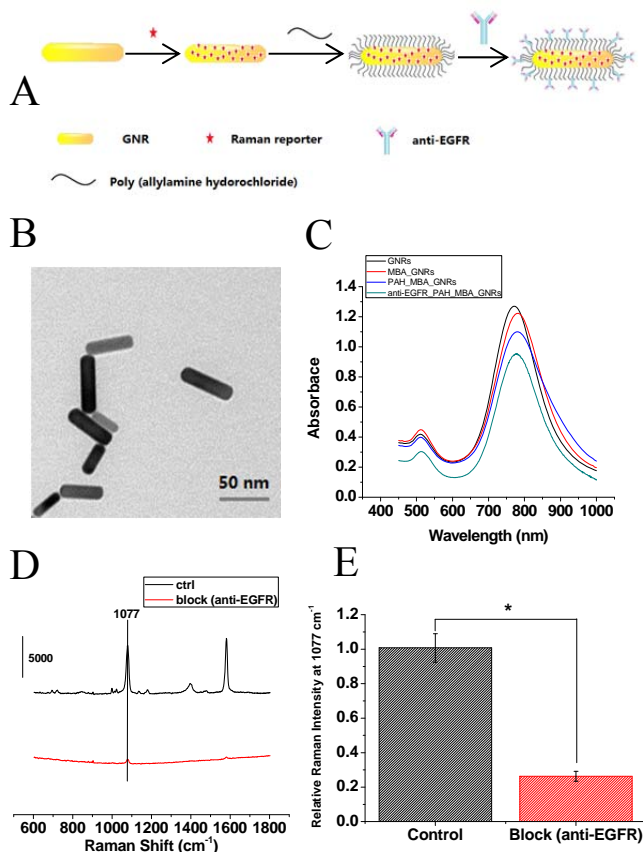


Fig. 1. (A) schematic illustration of the fabrication of the GNR-based, antibody-functionalized SERS probe. (B) TEM image of the SERS probe. (C) extinction spectra of the GNRs at each step of the coating process. (D) Typical SERS spectra and (E) normalized average Raman intensities ( $n = 60$ ) at  $1077\text{ cm}^{-1}$  for A431 cells (Control) and A431 cells pre-blocked by free anti-EGFR antibody molecules (Block).

In order to quantify how BRMS1 regulates the expression of EGFR in MDA-MB-435 (435) and MDA-MB-231 (231) cells, SERS measurement and western blot experiment have been carried out. As presented in Fig. 2B, BRMS1-transfected 435 cells ( $435^{\text{BRMS1}}$ ) have a significantly ( $P < 0.001$ ,  $n = 60$ ) lower level of EGFR expression than 435 cells, which overexpress EGFR; on the contrary, the transfection of BRMS1 doesn't have significant ( $P > 0.05$ ,  $n = 60$ ) effect on the expression of EGFR in 231 cells, which is EGFR positive. The exact mechanism of the selective effects of BRMS1 on EGFR expression in 435 and 231 cells remains unclear. However, these results—complete down-regulation of EGFR expression in 435 cells but no significant decrease in EGFR expression in 231 cells—are consistent with the results of traditional biological assay western blot (Fig. 2A). This shows that our designed SERS probe is capable of detecting the differences in EGFR levels between different cell lines.

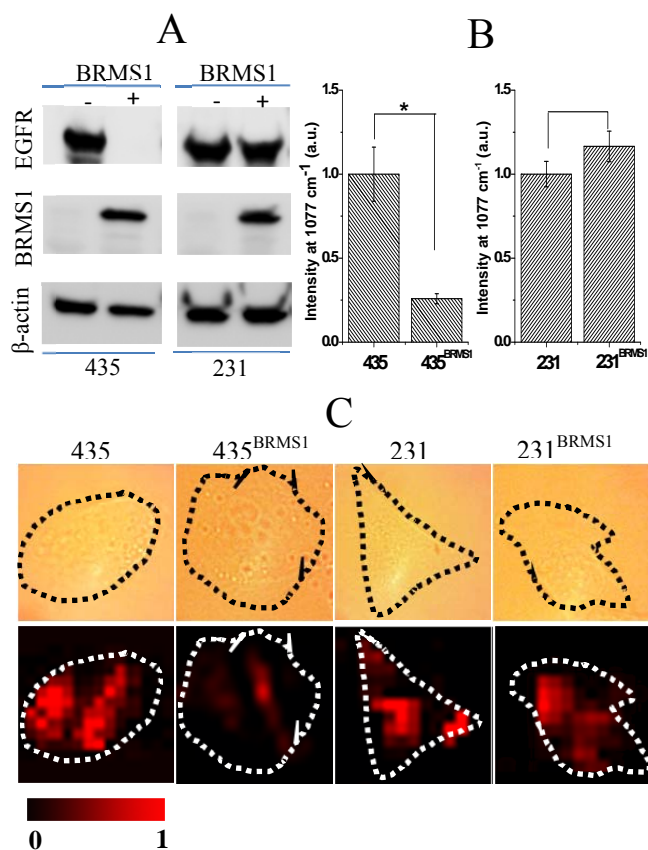


Fig. 2. (A) immunoblotting and (B) SERS detection of EGFR expression level regulated by the expression of BRMS1 gene in MDA-MB-435 and MDA-MB-231 breast cancer cells. (C) Bright field and SERS mapping ( $1077 \text{ cm}^{-1}$ ) images of 4 breast cancer cell lines: 435, 435<sup>BRMS1</sup>, 231 and 231<sup>BRMS1</sup>. The intensities were normalized between the lowest (0) and highest (1) color values for each pair of 435 vs. 435<sup>BRMS1</sup>, and 231 vs. 231<sup>BRMS1</sup>. Mapping size for all images is  $30 \times 30 \mu\text{m}^2$ .

To confirm the successful recognition of EGFR molecules and analyze their distribution on parental and BRMS1-expressing 435 and 231 cells, SERS mapping at  $1077 \text{ cm}^{-1}$  was performed on single cells in each cell line. The laser beam was focused on the surface membrane of single cells to image the interaction between SERS probes and EGFR molecules at cell surface. As shown in Fig. 2C, bright field images (upper panel) and their corresponding SERS mapping images (lower panel) were simultaneously recorded. These mapping images confirmed that the recognitions of EGFR were mostly at the cell surface and the receptors were heterogeneously distributed on the plasma membrane—mainly at the center of the cell, although still some receptors were located at the edge. In addition, SERS mapping once again verified the observation that the expression of BRMS1 down-regulated the EGFR in 435 cells, but had no significant influence in 231 cells.

### 3.2 TREC imaging of EGFR

Functionalization of AFM tips with anti-EGFR antibody was the key point to achieve successful TREC measurements. As shown in Fig. 3A, a procedure with 4 steps involved has been implemented to conjugate anti-EGFR monoclonal antibody with AFM tip to construct an EGFR-specific AFM nanosensor tip. It should be noted that, in this method, a PEG chain was applied to link the tip and the antibody due to its flexibility that allows for reorientation of the sensing molecule when the tip approaches the surface<sup>11</sup>. The morphologies of bare tip (Fig. 3B) and anti-EGFR antibodies modified tip (Fig. 3C) were characterized by scanning electron microscope (SEM). It is clearly seen that the morphology of modified probe was different from bare probe with the presence of “bumps” or “clusters” on the surface.

To evaluate the feasibility and efficiency of this TREC imaging method, we first chose mica as the substrate, since it's flat at atomic level and its much simpler circumstances than cell membrane surface. EGFR molecules were adsorbed onto the mica surface through electrostatic interaction. When anti-EGFR antibody-tethered AFM tip approached the surface and scanned through the surface, antibody-antigen recognition occurred, simultaneously generating maps of the surface topography (Fig. 4A) and recognition (Fig. 4B) signals. “Bright spots” on Fig. 4A represent single molecules or aggregates of EGFR, and the corresponding “dark spots” on Fig. 4B represent the recognition events of EGFR. These events were originated from the tip-tethered antibody binds to antigens, restricting the tip to oscillate upwards and leading to the reduction of the oscillation amplitude. To test the specificity of the recognition process, an anti-EGFR solution ( $20 \mu\text{g}/\text{mL}$ ) was injected via a liquid flow cell to block the interaction between tip-tethered anti-EGFR and EGFR on the surface. After 10 min adsorption, “dark spots” on recognition

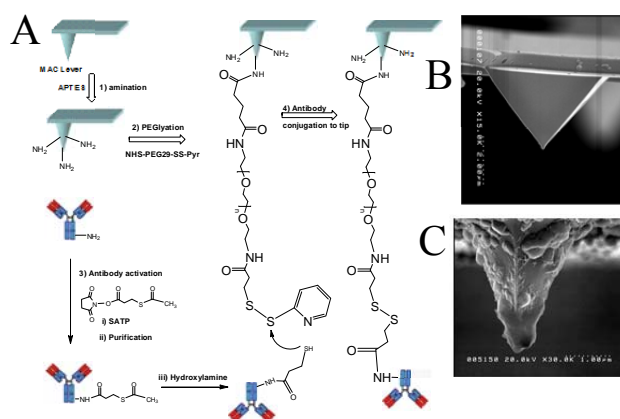


Fig. 3. (A) Fabrication AFM MAC lever: (1) MAC lever amination; (2) link MAC lever with PEG linker; (3) antibody activation by SATP; (4) SATP-antibody conjugate to AFM tip. (B) SEM image for bare tip. (C) SEM image for anti-EGFR functionalized tip.

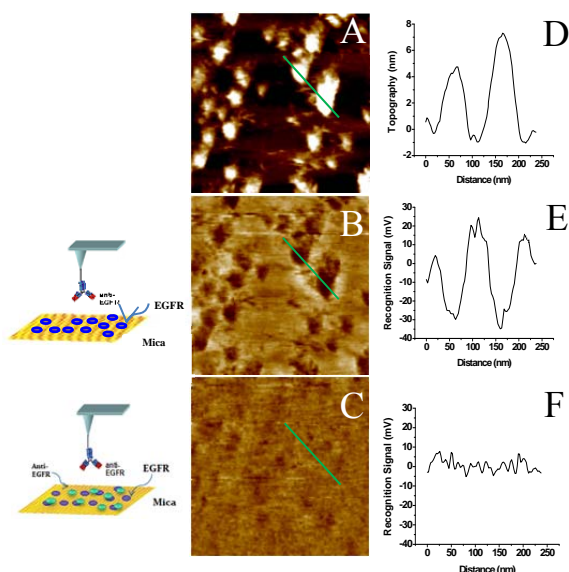


Fig. 4. Specificity of recognition. (A) Topographic image and (B) corresponding recognition image of EGFR on mica. (C) Recognition image of EGFR after blocking by free anti-EGFR. (D, E, F) Cross section analysis along the green line in (A, B, C). Scan area: 500nm\*500nm.

image were disappeared when conducting scan on the same location (Fig. 4C). Cross section analysis along the recognition (green lines on Fig. 4A, 4B, and 4C) showed that before free anti-EGFR blocking, there were significant recognition signals (Fig. 4E) corresponding to the topography signals (Fig. 4D), which indicated the height of molecules on the surface; however, as blocked by excess specific antibody, recognition signals of the antigens were dramatically decreased (Fig. 4F).

Finally, TREC imaging method was carried out to further probe the local distribution of EGFR molecules on the membrane surface of 435 and 435<sup>BRMS1</sup> cells (these two cell lines express EGFR at significantly different level). It is found that EGFR heterogeneously distributed on 435 cells and tended to form micro-domains (Fig.5A, 5B); with the expression of BRMS1, the numbers of EGFR binding sites reduced and smaller domains were observed (Fig.5C). The smallest “clusters” showing the recognition sites of EGFR molecules were nanometer scale, which is comparative to the size of single molecule of EGFR, indicating that TREC is able to achieve analysis of biomolecules at single-molecule level. Furthermore, the whole imaging process was done within several minutes, which means TREC imaging is capable of in situ monitoring many biological processes such as the activation of EGFR molecules by their specific ligands (e.g. EGF, TGF- $\alpha$ ).

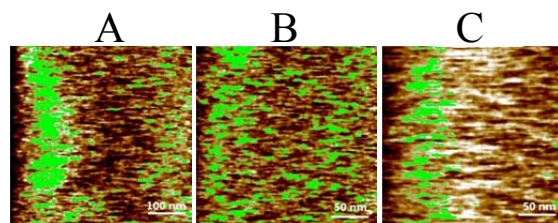


Fig. 5. Overlays of recognition images of EGFRs (green) onto corresponding topography images of 435 (A, B) and 435<sup>BRMS1</sup> cells (C).

## 4 CONCLUSION

We report a highly sensitive detection of breast cancer biomarker EGFR based on SERS and PicoTREC imaging techniques, which achieve the non-invasive detection of EGFR on cell surface membrane at single-cell and single-molecule levels.

We acknowledge the financial support from DoD award W81XWH-10-1-0668.

## 5 REFERENCES

1. Y. Yarden, *Eur J Cancer*, 2001, **37 Suppl 4**, S3-8.
2. J. Kneipp, H. Kneipp and K. Kneipp, *Chem Soc Rev*, 2008, **37**, 1052-1060.
3. R. A. Alvarez-Puebla and L. M. Liz-Marzan, *Small*, 2010, **6**, 604-610.
4. C. Stroh, H. Wang, R. Bash, B. Ashcroft, J. Nelson, H. Gruber, D. Lohr, S. M. Lindsay and P. Hinterdorfer, *P Natl Acad Sci USA*, 2004, **101**, 12503-12507.
5. D. B. DeWald, J. Torabinejad, R. S. Samant, D. Johnston, N. Erin, J. C. Shope, Y. Xie and D. R. Welch, *Cancer Res*, 2005, **65**, 713-717.
6. K. S. Vaidya, S. Harihar, P. A. Phadke, L. J. Stafford, D. R. Hurst, D. G. Hicks, G. Casey, D. B. DeWald and D. R. Welch, *J Biol Chem*, 2008, **283**, 28354-28360.
7. R. S. Samant, D. W. Clark, R. A. Fillmore, M. Cicek, B. J. Metge, K. H. Chandramouli, A. F. Chambers, G. Casey, D. R. Welch and L. A. Shevde, *Mol Cancer*, 2007, **6**, 6.
8. M. Cicek, R. Fukuyama, D. R. Welch, N. Sizemore and G. Casey, *Cancer Res*, 2005, **65**, 3586-3595.
9. M. M. Saunders, M. J. Seraj, Z. Li, Z. Zhou, C. R. Winter, D. R. Welch and H. J. Donahue, *Cancer Res*, 2001, **61**, 1765-1767.
10. Z. Novy, P. Barta, J. Mandikova, M. Laznicek and F. Trejtnar, *Nucl Med Biol*, 2012, **39**, 893-896.
11. C. K. Riener, C. M. Stroh, A. Ebner, C. Klampfl, A. A. Gall, C. Romanin, Y. L. Lyubchenko, P. Hinterdorfer and H. J. Gruber, *Anal Chim Acta*, 2003, **479**, 59-75.